LIMNOLOGY and OCEANOGRAPHY

ASLO

Limnol. Oceanogr. 65, 2020, 2984–2998

doi: 10.1002/lno.11569

A first assessment of cyanobacterial blooms in oligotrophic Lake Superior

Robert W. Sterner,[1*] **Kaitlin L. Reinl**,[1] **Brenda Moraska Lafrancois**,[2] **Sandra Brovold**,[1] **Todd R. Miller**[3]

[1]Large Lakes Observatory, University of Minnesota Duluth, Duluth, Minnesota
[2]National Park Service, Ashland, Wisconsin
[3]Zilber School of Public Health, University of Wisconsin-Milwaukee, Milwaukee, Wisconsin

Abstract

Lake Superior is often described as the most pristine of the Laurentian Great Lakes, but in the past decade *Dolichospermum* blooms have been observed. Land use in the adjacent watershed has not changed appreciably during this time, but the lake is warming and climatological variables correspond with presence of blooms. Blooms occurred only in relatively warm years as measured by degree days. Furthermore, the two largest blooms, in 2012 and 2018, occurred during years of especially extreme rainfall, providing coincidental evidence that intense storms provide nutrients or living propagules to the blooms from the watershed. Nearshore lake water in the narrow zone where blooms appear shows some riverine influence compared to water further offshore even in the absence of blooms. Nevertheless, water chemistry associated with the largest bloom in 2018 more closely resembled nonbloom nearshore lake water than river water, suggesting that blooms develop or at least persist outside of distinct river plumes. Concentrations of P and N during peak bloom density greatly exceeded any nonbloom lake or river waters, indicating that a buildup of phytoplankton biomass perhaps by floating and drifting to shore also is a significant factor in bloom occurrence. One potentially toxic substance (Anabaenopeptin A) was observed but at low concentration. At peak phytoplankton concentration, high seston C : P indicated severe P limitation while low C : N pointed against N limitation. If these newly observed blooms are indeed driven by temperature and rainfall as this evidence suggests, blooms may continue.

Cyanobacterial blooms (defined as "a massive accumulation of cyanobacterial biomass, formed through growth, migration, and physical–chemical forces"; Tromas et al. 2017) are a significant and increasingly prevalent global water quality problem (Paerl and Otten 2013; Ho et al. 2019). Blooms of cyanobacteria are most often associated with eutrophic or hypereutrophic lakes (Almanza et al. 2019), but they sometimes also occur in oligotrophic environments (Winter et al. 2011; Carey et al. 2012). Reasons frequently cited for the increased occurrence of cyanobacterial blooms include enhanced nutrient loading from watersheds and warming climate. The diversity of cyanobacterial species that produce blooms, and the complex set of interacting factors that drive them, make predicting and managing blooms challenging.

Earth's largest lakes are not immune to this global trend, with blooms known for Lakes Pontchartrain (Mishra and Mishra 2010), Taihu (Paerl and Otten 2013), Baikal (Namsaraev et al. 2018), and others. Blooms in large lakes are especially noteworthy because they are detrimental to ecosystem services that affect millions of people. The Laurentian Great Lakes (hereafter Great Lakes) are among the extremely large lakes of Earth that exhibit cyanobacterial blooms. Within the Great Lakes, previously described locations of blooms include Green Bay, Lake Michigan (Bartlett et al. 2018), Saginaw Bay, Lake Huron (Millie et al. 2008), and several locations in Lake Ontario including Bay of Quinte and Sodus Bay (Perri et al. 2015). The western basin of Lake Erie supports the largest and best-studied cyanobacterial bloom in the Great Lakes (Watson et al. 2016) and blooms are also occurring in the

*Correspondence: stern007@umn.edu

Additional Supporting Information may be found in the online version of this article.

Author Contribution Statement: All authors read and commented on manuscript drafts. R.W.S. was overall project lead and led the data analysis and writing for this contribution. K.L.R. assisted with field sampling, performed land use/cover analysis, and provided many comments on data interpretation. B.L.M. assisted with field work and project coordination and compiled information on historic bloom records. S.B. coordinated and performed day-to-day efforts in the field, maintained temperature sensors in the Apostle Islands, and generated the nontoxin chemical analytical data. T.R.M. provided the cyanotoxin data.

central Lake Erie basin (Chaffin et al. 2019). In all of these aforementioned Great Lakes blooms, watershed land-use factors are involved. In the western basin of Lake Erie, for instance, the Maumee River drains a region of high intensity row-crop agriculture and it enters into the shallow, partially hydrologically restricted western basin. The main source of water to Green Bay, the Fox River, is similarly a known major nutrient source (Bartlett et al. 2018).

Alone among the Great Lakes, Lake Superior has until now not been known to exhibit cyanobacterial blooms. But that has changed. In this article, we describe for the first time a newly recognized phenomenon where cyanobacterial blooms appear along the southern shore of western Lake Superior. Cyanobacterial blooms in Lake Superior are a surprise. The offshore is oligotrophic with chlorophyll generally < 1 μg L^{-1}. Phytoplankton growth is likely mostly P-limited (Sterner et al. 2004) due in part to a high (> 30 μmol L^{-1}) and continually climbing concentration of nitrate (NO_3^-) (Sterner 2011). The total N : P ratio (>300 by moles; Sterner 2011) is among the highest recorded for North American lakes. Lake Superior offshore summer phytoplankton are dominated by cyanobacteria by cell numbers but this is due to relatively high abundance of nonbloom-forming picocyanobacteria like *Synechococcus* and are diverse by biovolume with substantial contributions from diatoms, chrysophytes, cryptophytes, and dinoflagellates (Reavie et al. 2014; Bramburger and Reavie 2016). As described below, nearshore conditions do differ somewhat from the offshore.

In this article, we document some of the characteristics of Lake Superior cyanobacterial blooms and begin to address some of the potential factors promoting blooms.

Methods

Study site

The portion of Lake Superior from the Apostle Islands to the west is often referred to as the "western arm" of the lake (Fig. 1). The associated southern Lake Superior shoreline stretches ~ 100 km from its southwestern end at the Duluth-Superior harbor to its northeastern terminus at the Apostle Islands (Fig. 1, inset). The harbor is the lowermost expression of the St. Louis River Estuary, the largest (50 km^2) estuary in the Great Lakes (Bellinger et al. 2016). Both the St. Louis and the Nemadji Rivers drain into the harbor, which connects to the lake via two entries. The Superior entry at Wisconsin Point is the natural outlet of the harbor.

Lacking systematic, long-term quantification of phytoplankton biomass for the shoreline locations discussed here, we refer to a "bloom" as an event when dense phytoplankton populations were observed either suspended in the water or floating on the surface. Two widespread and readily observable Lake Superior cyanobacterial blooms are considered here to be "major" blooms because they were observed on more than 1 d or over more than one single location. On 14–15 July 2012 visitors reported to the National Park Service (NPS) at the Apostle Islands National Lakeshore (APIS) the presence of surface phytoplankton scums on beaches from Cornucopia, Wisconsin to Little Sand Bay (~ 20 km of shoreline) (https://www.wpr.org/green-scum-found-lake-superior; https://www.wnmufm.org/post/algae-found-lake-superior-wisconsin#stream/0; both last accessed 10 April 2020). The bloom was sampled on July 18, after it had somewhat abated. Quantitative phytoplankton counts were not performed, but *Dolichospermum lemmermannii* (formerly, *Anabaena lemmermannii*) was identified as the most abundant phytoplankton species (Gina LaLiberte, Wisconsin Department of Natural Resources) (Supporting Information Fig. S1A). Samples from the 2012 bloom submitted to the USGS Organic Geochemistry Research Laboratory at the Kansas Water Science Center for toxin screening showed microcystin concentrations below detection limits of 0.1 μg L^{-1}. No other chemical or biological data of the bloom were taken at that time.

The other, much larger, major bloom was first reported to NPS staff on the afternoon of 09 August 2018 by visitors to the Meyers Beach access point to Mawikwe Bay and the Sea Caves areas. Bloom conditions were also observed by NPS staff and public beach-goers at nearby Cornucopia Beach later that afternoon (Supporting Information Figs. S1D, S2). Over the subsequent week, bloom conditions were reported from points ranging from the Twin Ports of Duluth/Superior, in far western Lake Superior, to the easternmost Apostle Islands (a shoreline span of > 100 km). Satellite imagery (Fig. 2) indicates that the bloom primarily occupied the nearshore at ≤ 0.5 km from shore.

Other documented observations of cyanobacterial blooms for Lake Superior were at only a single point location on a single day, and thus are referred to here as "minor" blooms. These include surface scums at the Sea Caves on 31 August 2016 (https://www.wpr.org/blue-green-algae-spotted-again-lake-superior, last accessed 21 April 2020) and 09 August 2017. *D. lemmermannii* were dominant in both (Supporting Information Fig. S1B,C). Both heterocysts and akinetes have been observed in blooms of *Dolichospermum* in Lake Superior, but neither have been quantified.

The St. Louis River Estuary has a long history of human impact and subsequent recovery (Bellinger et al. 2016; Alexson et al. 2018). Installed in 1978, the Western Lake Superior Sanitary District (WLSSD) is a tertiary wastewater treatment plant serving Duluth, MN and surrounding communities that discharges into the harbor. Bellinger et al. (2016, fig. 2)) show a decrease in total phosphorus (TP) concentration of roughly 10-fold and a decrease in total suspended solids (TSS) concentration of roughly fivefold between 1960 and 2010 while dissolved oxygen (DO) concentration in the thalweg approximately doubled over the same period (their fig. 3). The only drinking water intake on this stretch of shoreline is the City of Superior, WI, which serves 10,000 customers and draws water from ~ 3 m below the sand–water interface at the bottom of the lake offshore of the city. At the eastern end of

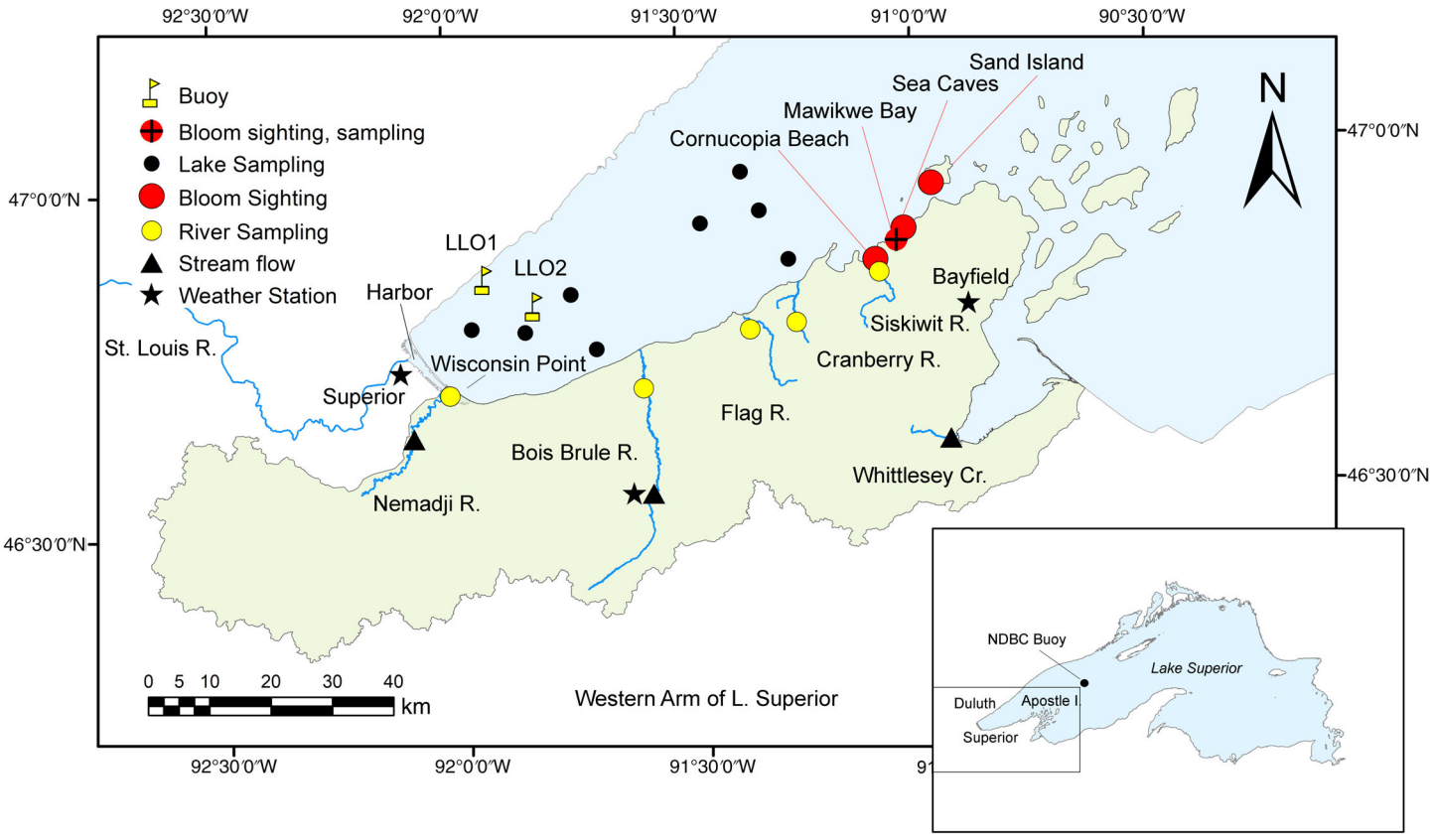

Fig. 1. Map of relevant locations in the western arm of Lake Superior. The portion of the watershed where land use was examined is shaded in light green. Rivers where sampling was performed are labeled in blue. Latitude/longitude of locations are given in Table 2.

Fig. 2. RapidEye Ortho Tile (5 m) image of the Lake Superior south shore from approximately Wisconsin Point to the Brule River (Fig. 1) from 09 August 2018 (Planet Team 2017), color-enhanced to emphasize bloom.

this study region, large portions of the Apostle Islands and nearby mainland are protected as national and tribal parklands, state natural areas, and national, state, county, and tribal forestlands. The southern shore of Lake Superior is shallower (Supporting Information Fig. S3) and warmer (Xue et al. 2015) than the north shore. Hydrodynamic modeling indicates a summer residence time of 20–60 d in the southern nearshore zone of the western arm (Mckinney et al. 2018). Some detailed cross sections from N to S in the western arm of temperature, backscatter, chlorophyll fluorescence, Chromophoric Dissolved Organic Matter (CDOM), and DO are presented in Austin (2013), which also shows sediment resuspension occurring in the southern nearshore. The western arm typically exhibits greater autotrophy (Russ et al. 2004)

than the bulk of the lake to the east, presumably because it is shallower, warmer, and is river-influenced. The nearshore (20 m depth contour) in this portion of the shoreline has lower light penetration, higher conductivity, chlorophyll fluorescence, and zooplankton biomass than the rest of the U.S. shore (Yurista et al. 2011). This location also experiences significant storm-derived sediment plumes due to its geologic setting (Minor et al. 2014; Cooney et al. 2018).

Percent land cover for this portion of the watershed (Fig. 2) was calculated using ArcMAP 10.4 and the USGS National Land Cover Dataset for 2001, 2006, 2011, and 2016 (Yang et al. 2018) (Table 1). Land cover is > 75% forest or woody wetlands. Agriculture's largest footprint is in Pasture/Hay with cultivated crops making up < 1% of land area. Developed land also makes up < 1% of the land area. There are no obvious shifts in land uses that suggest new large nutrient sources to the lake (Table 1). The predominance of glaciolacustrine red clay deposits in this portion of the watershed—together with differential isostatic rebound (more rapid to north and east), which causes submergence of this stretch of shoreline—make the southern shore of the western arm an important source of sediment and nutrients to Lake Superior (Kemp et al. 1978; Robertson 1997). The mineralogy of these clays causes P to be tightly bound to the sediment entering the lake (Tonello et al. 2019), reducing the immediate bioavailability of P associated with clay particles. The ultimate fate of P entering the lake on these clay particles is not yet known.

Temperature

The longest span of surface-water temperature observations for western Lake Superior (since 1981 with no data reported for 2007) comes from a National Data Buoy Center (NDBC)-maintained buoy northeast of the Apostle Islands (Table 2).

Table 1. Land Cover (percent of area) in the Lake Superior watershed from the Nemadji River around the Bayfield peninsula (Fig. 1) for 4 yr, per the National Land Cover Dataset from USGS.

ID	2001	2006	2011	2016
Deciduous or Mixed Forest	54.3	53.6	57.1	56.6
Woody Wetlands	12.3	12.2	9.1	15.6
Evergreen Forest	10.9	10.8	10.8	8.2
Pasture/Hay	7.7	7.9	7.5	8.2
Shrub/Scrub	6.7	6.8	6.3	2.8
Developed, Open Space	4.1	4.1	4.3	3.2
Open Water	1.4	1.4	1.3	1.2
Grassland/Herbaceous	0.4	0.9	1.6	1.2
Emergent Herbaceous Wetlands	0.8	0.8	0.4	1.5
Cultivated Crops	0.7	0.7	0.6	0.6
Developed, Low Intensity	0.5	0.5	0.5	0.5
Developed, Medium Intensity	0.1	0.1	0.2	0.2
Barren Land (Rock/Sand/Clay)	0.0	0.1	0.1	0.2
Developed, High Intensity	0.0	0.0	0.1	0.0

This location is quite distant from the area of the lake susceptible to blooms but is included here to provide offshore context. As will be shown later, the nearshore where blooms occur is often warmer than this location, especially early in the summer. Two other buoys (LLO1 and LLO2) are closer to the locations of observed blooms (Fig. 1) and have been maintained by the Large Lakes Observatory since 2011. Buoys report temperature at 0.6 m (NDBC) or 1 m (LLO) water depth every hour (NDBC) or every 10 min (LLO). In addition, sensor-based observations of water temperatures have been made for some periods since 2015 by the authors and their University of Wisconsin-Milwaukee collaborators at Sand Island, APIS (Fig. 1). Here, sensor temperatures have been converted to daily averages. We also calculated degree days (DD) each year as the cumulative sum of daily surface temperature > 10°C for the two LLO buoys averaged (or for a single buoy when data for only one was available). This baseline temperature was chosen because some buoy deployment dates meant some years were lacking sufficient surface temperature observations < 10°C.

Hydrology

We obtained daily precipitation records for three currently operating National Weather Service Cooperative stations (Fig. 1, data downloaded on 17 January 2019 from https://mrcc.illinois.edu/CLIMATE/welcome.jsp). To obtain an indication of rainfall across this part of the shoreline, we added the values for the three stations together for a summed value (averages would simply be divided by three). We also examined streamflow data for locations near these three weather stations (Fig. 1, data downloaded on 21 January 2019 from https://waterdata.usgs.gov/nwis/rt). Of these three gauged stations, the Nemadji River represents the largest catchment area (1088 km^2), with the Bois Brule River (306 km^2) and Whittlesey Creek (20 km^2) being smaller. To gain an understanding of river flow across the watershed, we examined each of the three watersheds separately rather than adding or averaging them, which would have greatly emphasize the larger watersheds.

Field sampling

In 2017, six locations were sampled at approximately 3-week intervals from May 31 to October 05 (Fig. 1; Table 2). Sites included three river (Bois Brule, Flag, Siskiwit), one harbor outflow (Wisconsin Point), and two nearshore lake stations near APIS (Sand Island and Mawikwe Bay, adjacent to Meyers Beach). An opportunistic sample based on bloom report for phytoplankton community identification was also taken in 2017 in the nearshore at the Sea Caves site. In 2018, the Sand Island and Wisconsin Point stations were dropped and a Cranberry River station was added. The sampling frequency was increased to every other week from 23 May 2018 to 26 September 2018 totaling 14 sampling dates. In addition, opportunistic sampling associated with the August 2018

Table 2. Data sources, their spatial coordinates, and years when data were available. See Fig. 1 for a map.

	Location	Lat. (°N)	Long. (°W)	Years data available*	Notes
Buoys	LLO1 (NDBC 45027)	46.860	91.932	2011–2018	Surface temp; https://www.ndbc.noaa.gov/station_page.php?station=45006
	LLO2 (NDBC 45028)	46.818	91.828	2011–2018	Surface temp; https://www.ndbc.noaa.gov/station_page.php?station=45028
	NDBC 45006	47.335	89.793	1981–2018	Surface temp; https://www.ndbc.noaa.gov/station_page.php?station=45027
Weather stations	Superior	46.727	92.072	1909–2018	Precipitation
	Brule Ranger Station	46.538	91.592	1828–2018	Precipitation
	Bayfield Fish Hatchery	46.787	90.864	2006–2018	Precipitation
Stream flow	Nemadji River, USGS 04024430	46.633	92.094	1973–2018	Flow
	Bois Brule River, USGS 04025500	46.538	91.595	1942–1981, 1984–2018	Flow
	Wittlesey Creek USGS 040263205	46.594	90.963	1999–2018	Flow
Offshore	LCCMR 1	46.780	91.849	2014–2016	Water chemistry
	LCCMR 4	46.788	91.962	2014–2016	Water chemistry
	LCCMR 5	46.998	91.376	2014–2016	Water chemistry
	LCCMR 6	46.940	91.341	2014–2016	Water chemistry
	LCCMR 7	46.867	91.284	2014–2016	Water chemistry
	LCCMR 9	46.926	91.467	2014–2016	Water chemistry
	LCCMR 11	46.832	91.7490	2014–2016	Water chemistry
	LCCMR 12	46.751	91.700	2014–2016	Water chemistry
Nearshore	Mawikwe Bay	46.886	91.053	2017–2018	Includes several locations within 0.4 km of indicated coordinates; Water chemistry
	Sand Island West	46.966	90.972	Temp: 2015–2018 Chem: 2017	Bloom sighting; Water temperature
	Sand Island East			Temp: 2015–2017 Chem:	Water temperature
	Cornucopia Beach	46.860	91.100	August 2018	Bloom sighting; Water chemistry
	Sea Caves	46.903	91.036		Bloom sighting
	Herbster Beach				Bloom sighting
Rivers	Wisconsin Point	46.707	92.013	2017	Water chemistry
	Bois Brule	46.705	91.604	2017–2018	Water chemistry
	Flag	46.782	91.372	2017–2018	Water chemistry
	Cranberry	46.789	91.273	2018	Water chemistry
	Siskiwit	46.855	91.092	2017–2018	Water chemistry

*Not all years used for analysis.

bloom was performed at various locations in this region. Water samples were collected in the lake from a boat and at the river and harbor stations via a bridge, pier, or when possible from shore. Surface water was collected from the surface into clean 8- or 20-liter carboys using a clean bucket. Samples for algal toxins and TP were collected into separate bottles.

For an offshore lake comparison of water chemistry, we utilize data collected from 11 cruises conducted in 2014–2016 (dates ranging from May to October) using the R/V *Blue Heron* (Table 2; Fig. 1). Water was obtained using Niskin bottles. Here, we use data collected from water depth ≤ 20 m with the majority coming from ≤ 5 m.

Analytical methods

Water was filtered through 25 mm preashed GF/F filters for particulate organic carbon (POC) and nitrogen (PON), through 25 mm preashed, acid-rinsed GF/F filters for particulate phosphorus (PP), and through 25 mm 0.2 μm cellulose nitrate

filters for chlorophyll *a* (Chl *a*). Total dissolved phosphorus Total dissolved phosphorus (TDP) and soluble reactive phosphorus (SRP) measurements were made on 0.22-μm filtered samples. Subsamples for the dissolved analytes were prefiltered through 0.45 μm capsule filters then through a 47 mm 0.2 μm filter. Postfiltration, all samples were preserved immediately by freezing at −4°C (most analytes), drying at 60°C (POC and PON), or by acidification to a pH of 2 (dissolved organic carbon [DOC]).

Samples for phytoplankton community analysis were taken in 2017 in river and lake sites. Whole water was preserved with Lugol's and transferred to D. Perkins at the Wisconsin State Laboratory of Hygiene (Madison, WI) where they were analyzed in a settling chamber using an inverted phase contrast microscope at ×630 magnification following 10200F1 (Counting Units) and 10200F2c1 (Inverted Microscope counting procedures) from APHA Standard Methods (2012) where for colonies, cells falling within sampling fields were counted. Phytoplankton were identified to genus and a minimum of 300 natural units (cells or colonies) were thus enumerated. Chl *a* was analyzed using a Turner Design 10-AU fluorometer, calibrated yearly with NIST liquid Chl *a* standards and daily with solid standards, using the Welschmeyer (1994) method following an overnight acetone extractions. POC and PON were analyzed on a Costech Elemental Analyzer. PP, TP, SRP, and TDP samples were analyzed on a SEAL AQ400 following where needed a potassium persulfate digestion modification of EPA method 365.1. NO_3^- and silicate were also run on a SEAL AQ400 using EPA method 353.2 and Standard Methods 4500-SiO_2, respectively. Total organic carbon (TOC), DOC, and total dissolved nitrogen (TDN) were run on a Shimadzu TOC-Vcsh with a TNM-1 module. Total nitrogen (TN) was calculated from PON + TDN. Ammonia was run using the Taylor et al. (2007) method or for samples that exceeded the acceptable range for this method on the SEAL AQ400 using EPA method 350.1.

Water samples were analyzed for 22 cyanobacterial toxins in six classes: 11 microcystins (MCs), nodularin (NOD), 3 anabaenopeptins (Apts), 3 cyanopeptolins (Cpts), microginin-690 (Mgn690), anatoxin-a (ATX) and homoanatoxin-a (hATX), and cylindrospermopsin (Cyl). Analysis used liquid chromatography tandem (MS/MS) mass spectrometry with electrospray ionization (Beversdorf et al. 2017). MCs, NOD, Apts, Cpts, and Mgn690 were extracted in acidified 70% methanol after lyophilization of a 30 mL aliquot (Beversdorf et al. 2017). For ATX, hATX, and Cyl, a 10 mL aliquot was lyophilized to dryness and extracted with acidified water using sonication (Beversdorf et al. 2017). Whenever possible, certified reference materials were used. MCLR and desmethyl-MCLR (Dha7-MCLR) were purchased as certified reference materials from the National Research Council of Canada Biotoxins program (Halifax, Nova Scotia, Canada). NOD (purity > 94%), MCLA (> 95%), MCYR (> 90%), and MCRR (> 90%) were purchased from Sigma-Aldrich (Milwaukee, Wisconsin, U.S.A.), and CYL (> 95%) was purchased from Abraxis (Warminster, Pennsylvania, U.S.A.). For the peptides, AptB (> 95%) and AptF (> 95%), Cpt1007 (> 95%), Cpt1021 (> 95%), Cpt1040 (> 95%), and Mgn690 (> 95%) were purchased from Marbionc (Wilmington, North Carolina, U.S.A.). Additionally, ATX fumarate (96%) was purchased from Tocris Bioscience (Minneapolis, Minnesota, U.S.A.) as a racemic mixture, and hATX (> 95%) was purchased from Abraxis.

Results

Phytoplankton community composition

Routine samples for phytoplankton community composition taken from the rivers and the nearshore from May–October 2017 (Supporting Information Fig. S4) indicated a strong predominance of Bacillariophyta (multiple genera) and Cryptophyta (principally *Komma*). The nearshore lake community also included Chrysophyta (principally *Dinobryon*) and Chlorophyta (principally *Golenkinia*) (Supporting Information Fig. S4A,C). Small numbers of Euglenophyta (principally *Strombomonas*) were observed occasionally. Picocyanobacteria could not be detected with these methods and larger, observable, cyanobacteria (principally *Aphanizomenon*) were recorded only at Wisconsin Point where the harbor enters the lake (Supporting Information Fig. S4G) and, notably, in high dominance in the opportunistic sample taken of the minor bloom observed at the Sea Caves nearshore site in August (> 80% *Dolichospermum*) (Supporting Information Fig. S4E). Seasonal patterns at this level of taxonomic resolution were not easily discerned. These results underscore the usual rarity of larger cyanobacterial taxa in this system.

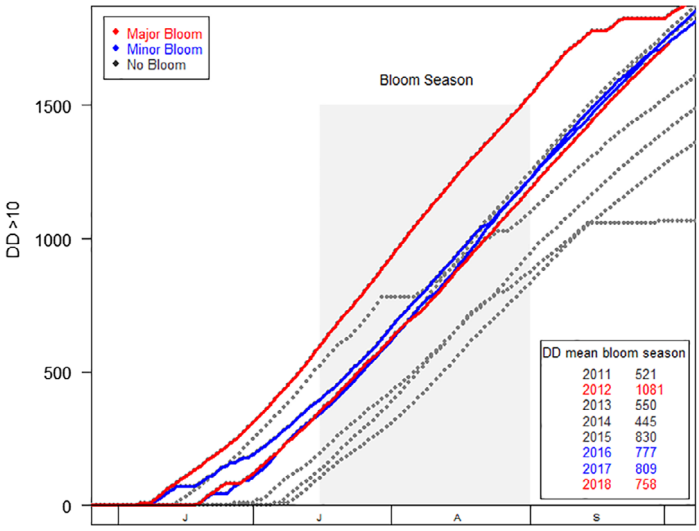

Fig. 3. Degree days (> 10°C) on a given day of the year for 2011–2018. Bloom years are shown in color and the season over which blooms have been observed in the past is shaded in gray. The table at lower right provides the mean DD during the shaded bloom season for each year. More detailed temperature data are given in Supporting Information Fig. S5.

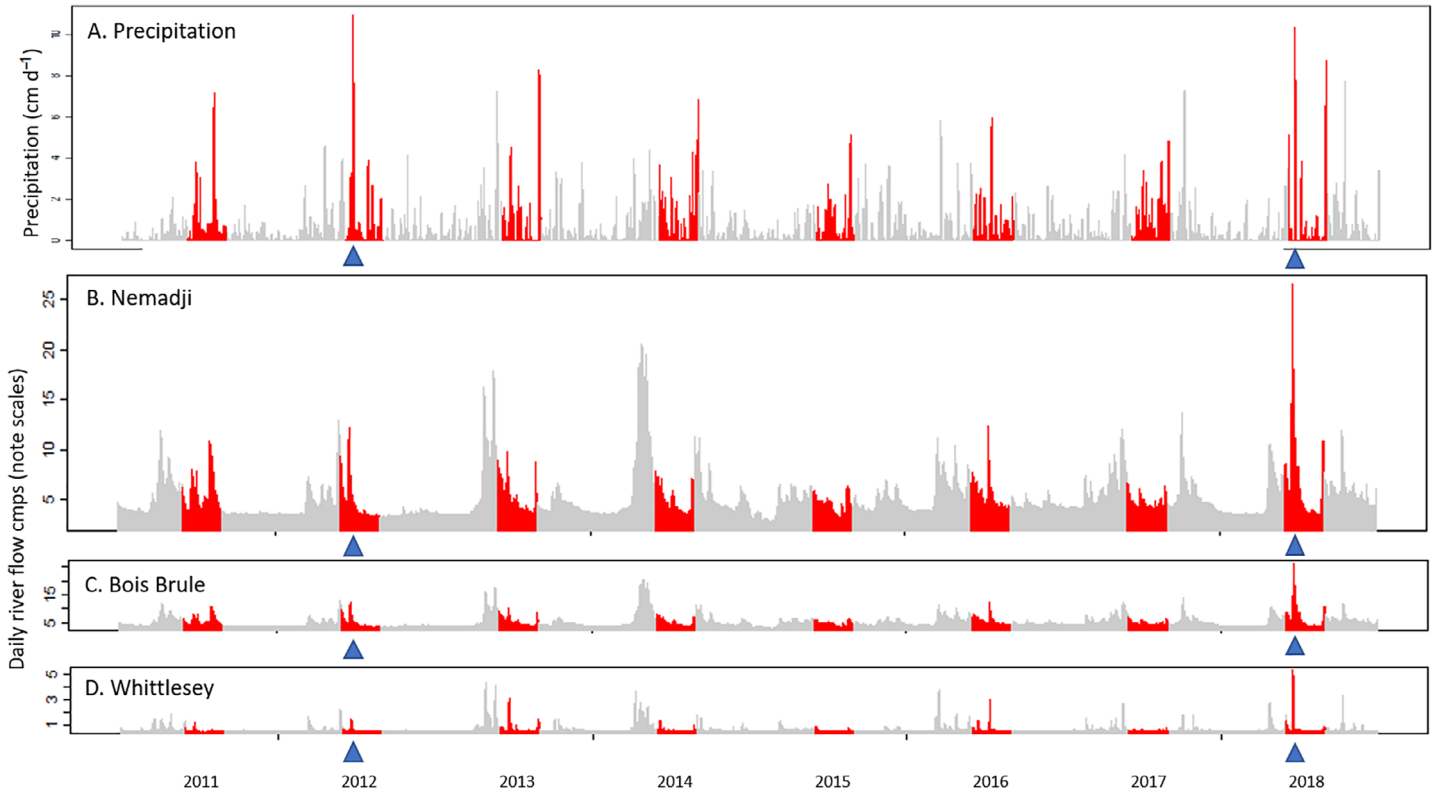

Fig. 4. Precipitation (**A**), and stream flow (**B**–**D**) in the study region (3-d moving averages and with June, July, and August shown in red). (**A**) Rainfall (cm d^{-1}) summed for three weather stations indicated in Fig. 1. (**B**–**D**) Streamflow (m^3 s^{-1}) for three individual gauged stations indicated in Fig. 1. The 2012 and 2018 storm events are indicated with blue triangles.

Table 3. Top five events for rainfall (sum of three stations) and for flow for each of the three representative watersheds. Values are 3-d moving averages centered on the date indicated.

Rainfall		Nemadji		Bois Brule		Whittelsey	
Date	cm	Date	m^3 s^{-1}	Date	m^3 s^{-1}	Date	m^3 s^{-1}
20 Jun 12	4.31	18 Jun 18	367	18 Jun 18	26.5	16 Jun 18	5.39
19 Jun 12	4.3	21 Jun 12	344	19 Jun 18	24.5	17 Jun 18	4.87
16 Jun 18	4.07	17 Jun 18	309	17 Jun 18	21.2	18 Jun 18	4.71
27 Aug 18	3.45	20 Jun 12	307	20 Jun 18	20.8	28 Apr 13	4.35
26 Aug 13	3.26	03 Aug 11	295	01 May 14	20.5	29 Apr 13	4.21
27 Aug 13	3.16	19 Jun 18	269	02 May 14	20.3	21 May 13	4.1

Temperature

Seasonal surface temperature patterns recorded by the buoys exhibit short-term (days to weeks) variability superimposed on annual warming and cooling patterns as a result of meteorology as well as mixing patterns in the lake (Supporting Information Fig. S5). Surface temperature in the western arm (Supporting Information Fig. S5, red, blue, black) rises faster in the spring than in the far offshore (Supporting Information Fig. S5, gray), and it warms slightly earlier in the Spring within the Apostle Islands (Supporting Information Fig. S5, black, 2016 and 2017) than elsewhere in the western arm (Supporting Information Fig. S5, blue, red). By June, however, surface temperatures within the Apostles are similar to the rest of the western arm (note correspondence of black to red and blue points in Supporting Information Fig. S5), so that the two LLO buoys provide reasonable information about the surface temperatures on the south shore during cyanobacterial blooms. Further analysis of temperature thus is based on the

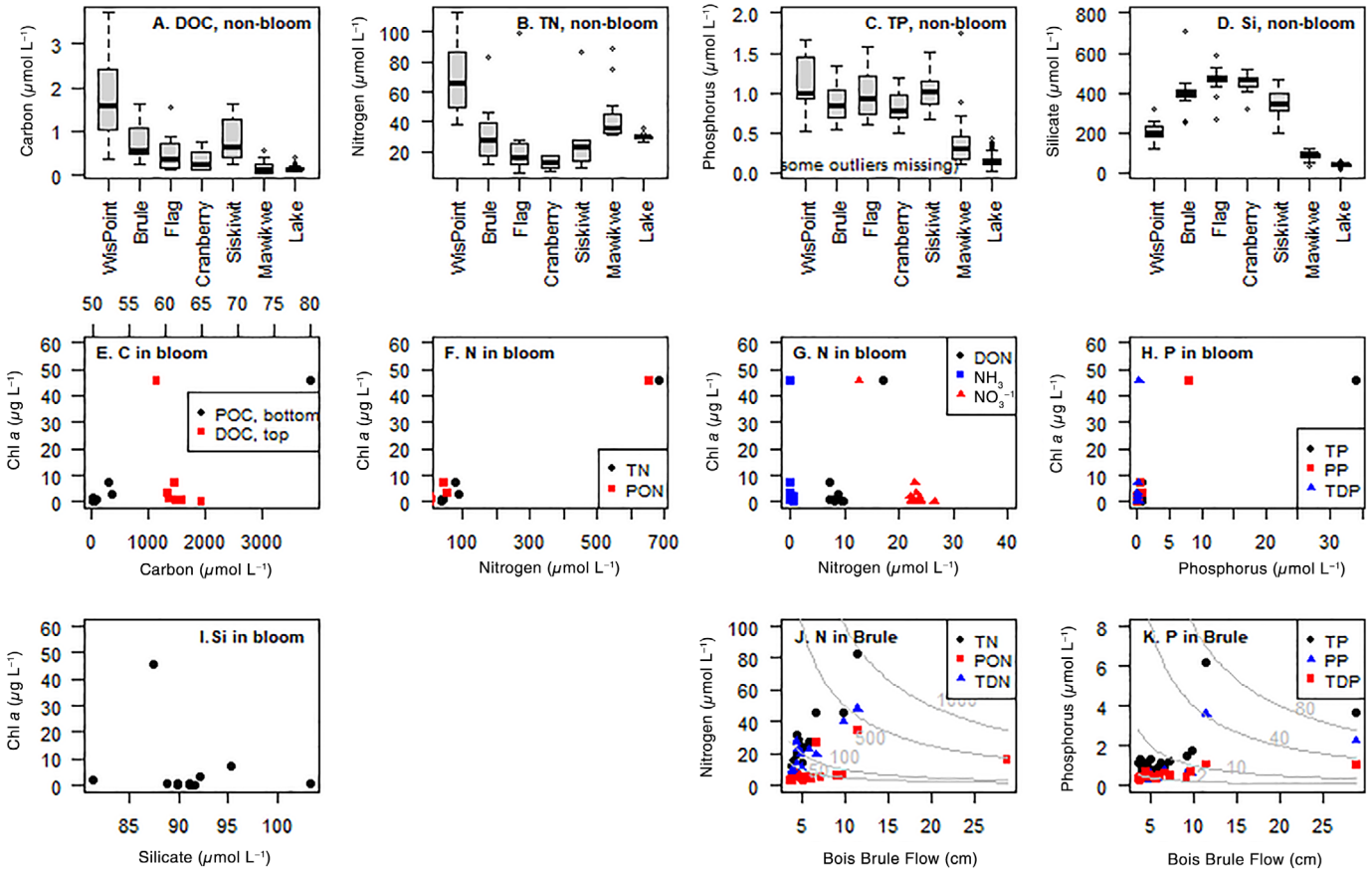

Fig. 5. Dissolved and particulate elements. Boxplots (**A**–**D**) show various sampling locations excluding the August 2018 bloom (so referred to here as "nonbloom") with medians as horizontal bars along with first and third quartiles indicated by rectangles and the full data range as whiskers, and with individual outliers plotted when they fall > 1.5 times the interquartile range. (**A**) DOC. (**B**) Total nitrogen (sum of TDN and PON). (**C**). TP. (**D**). Dissolved silicate. Scatterplots (**E**–**I**) show chlorophyll in August 2018 nearshore samples including the bloom vs. various element fractions. (**E**) POC and DOC. (**F**) Total nitrogen and PON. (**G**) Dissolved organic nitrogen, ammonia (NH_3), and nitrate (NO_3^-). (**H**) TP, PP, and TDP. (**I**) Dissolved reactive silicate. TN in the Bois Brule River vs. flow. Bois Brule loading plots (**J**, **K**) show individual sampling points as well as gray curves that represent equal loading rate (mmol s^{-1}). (**J**) Nitrogen. (**K**) Phosphorus. See Table 4 for associated statistics.

mean surface temperature observed at the two LLO buoys on any given day of the year.

Seasonal peak surface temperatures across all years ranged only from 19.8°C (2014) to 23.9°C (2015). Similarly, surface temperatures observed ± 5 d of observed blooms also varied comparatively little, from 19.6°C (2017) to 23.5°C (2012). Seasonal patterns of warming, however, showed more variation from year to year. Analysis of DD revealed that years with either major or minor blooms were at the high end of the range of DD for a given day of the year (Fig. 3). Warm years typically reached the 10°C baseline earlier in the year than cold years (Fig. 3). Mean DD during the season in which blooms occur (*see* Fig. 3) was higher in years with vs. without blooms (Welch two-sample, one-tailed t = 2.38, df = 5.93, p = 0.028). The nonbloom years 2011, 2013, and 2014 were unambiguously cold in terms of DD, and all four bloom years (2012, 2016–2018) were unambiguously warm (Fig. 3). The year 2015 is more difficult to characterize in that it exhibited rapid early season warming, but then also rapid and unusual cooling in late July/early August (Supporting Information Fig. S5). Overall, with recognition that the number of years examined here is not large, these data suggest that early and sustained seasonal warming is associated with *Dolichospermum* blooms in Lake Superior.

Hydrology

Lake level ranged widely over 2011–2018 from an annual mean of 183.09 m (2011) to 183.63 m (2017), or roughly two thirds of the entire historic range of 182.94 (1926) to 183.73 (1986) (data from www.glerl.noaa.gov). Lake level was below the long-term average from 2011 to 2013 and above it from 2014 to 2018. Peak river flows occurred in some years along with high rainfall events but in other years they occurred early in the year in the absence of significant rainfall, and thus

likely included significant snowmelt (Fig. 4). Most large rainfall events in this region occur between June and August (Fig. 4), and the two largest rainfall events from 2011 to 2018 occurred in June of 2012 and 2018 (Table 3). Our sampling of the Bois Brule River included the highest daily flow observed during 2017–2018 and thus captured the major rainfall event of 2018. The June 2018 rainfall event produced the highest observed flows from 2011 to 2018 in all three rivers. The June 2012 rainfall event was unusually high mainly in the western part of this watershed as the rainfall was most concentrated over the Duluth, MN (Cooney et al. 2018), as indicated by flows in the Nemadji River, but the storm clearly affected all three rivers. The 2012 and 2018 events both had 1/500 or smaller annual exceedance probabilities in the locations where rainfall was heaviest (data provided by the Duluth National Weather Service). One other rainfall event between 2011 and 2018 (in mid-July, 2016) had similarly low exceedance probabilities but its heaviest rainfall fell outside of the watershed area studied here. The 2012 cyanobacterial bloom occurred 25 d after the major June rainfall of that year and the 2018 bloom occurred 53 d after that year's major rainfall event.

Carbon and nutrients

We examined carbon and nutrient data in three principle ways. First, we summarized the measurements across 2017–2018 made at the harbor entry (Wisconsin Point), in the rivers, and the near- and off-shore of the lake. This provided a way to see how lake chemistry in and out of blooms related to inflowing river chemistry. Second, we looked to see how chlorophyll varied with different chemical parameters in the nearshore of the lake between the Bois Brule River and the Sea Caves between 03 August 2018 and 27 August 2018; this allowed us to describe the carbon and nutrient dynamics directly associated with major bloom peak and collapse. Third and last, we explored the impact of varying river flow on chemical concentrations and nutrient loading by plotting observed concentrations in the gauged Bois Brule River as a function of flow over the full 2017–2018 observation period. Other rivers lacked comprehensive flow data. This allowed us to see how river flow conditions affected loading of nutrients to the lake.

DOC was higher in the rivers than in the lake, with Wisconsin Point showing highest DOC and some variation among the other rivers (Fig. 5A). DOC was not statistically significantly related to river flow (Table 4). DOC showed a small but significantly negative relationship with chlorophyll (Fig. 5E; Table 4), remaining below 70 μmol L^{-1}. The lowest DOC concentration in any of the rivers at any point in 2017–2018 (~ 1.5 mg L^{-1}) exceeded the DOC concentration observed in the nearshore in August 2018 by greater than twofold. POC was positively associated with chlorophyll during the 2018 bloom month (Fig. 5E; Table 4).

TN also was highest at Wisconsin Point (Fig. 5B). DON, NO_3^-, and PON all contributed substantially to this total (not shown). Lake NO_3^- concentrations in excess of 30 μmol L^{-1} caused lake TN to exceed TN observed in any of the other rivers (Fig. 5B). The peak bloom exhibited a far higher TN than seen in any river or lake sources in this part of the

Table 4. Spearman rank correlations (ρ) for August 2018 nearshore, lake samples (parameter vs. chlorophyll) and for 2017–2018 Bois Brule River samples (parameter vs. Bois Brule River flow for that day).

		Chlorophyll, Aug 2018			Bois Brule River Flow, 2017–2018		
		Spearman ρ	*n*	*p*	Spearman ρ	*n*	*p*
Total	TN	0.71	8	0.046	0.73	11	0.011
	TP	0.77	11	0.005	0.55	21	0.0099
Particulate	Chlorophyll	—	—	—	0.76	21	<0.0001
	POC	0.64	11	0.035	0.66	21	0.001
	PON	0.77	11	0.005	0.67	21	0.0001
	PP	0.82	11	0.002	0.74	21	0.0001
	C:P	0.62	11	0.043	−0.34	21	0.13
	N:P	0.82	11	0.002	−0.27	21	0.24
	C:N	−0.85	11	0.008	0.14	21	0.55
Dissolved	DOC	−0.86	8	0.006	0.53	11	0.096
	DON	−0.05	8	0.92	0.68	7	0.094
	TDN	−0.83	8	0.01	0.65	11	0.032
	NH_3	−0.46	11	0.15	0.66	21	0.0011
	NO_3^-	−0.56	11	0.071	0.46	17	0.063
	TDP	0.25	11	0.47	0.70	21	0.0004
	SRP	0.02	11	0.96	0.20	21	0.39
	Si	−0.10	11	0.77	−0.48	19	0.037

lake—during the August 2018 bloom, TN was approximately 700 μmol L^{-1} above the nonbloom background Fig. 5F), with the vast majority of this nitrogen in the form of PON (Fig. 5F). Although TDN was significantly lower with chlorophyll in the nearshore during the period, the other forms of dissolved N were not significantly related to chlorophyll (Fig. 5G; Table 4). TN, TDN, and PON in the Bois Brule River increased with flow such that the storm-related TN loading rate to the lake was approximately 20 times higher than at base flow (Fig. 5J).

TP at Wisconsin Point (mean = 1.3 μmol L^{-1}) and in all the rivers were roughly consistent, and were higher than in the nearshore or offshore (Fig. 5C). Both TP and PP rose considerably during the bloom while TDP remained low (Fig. 5H). The high observed value of TP at peak bloom exceeded the sum of PP and TDP at that time, but we could not ascertain why. A small amount of particles between 0.2 and 0.7 μm would be missed in the sum of PP and TDP compared to TP, but this is highly unlikely to account for this inconsistency. We searched for any effect of turbidity, incomplete digestion, or inconsistent results upon rerunning these samples and could find no sources of error. TP, TDP, and PP, but not SRP, increased with flow rate in the Bois Brule River (Table 4) such that the storm-related TP loading rate to the lake was ~ 30× higher than at base flow (Fig. 5K). Dissolved silicate remained within a limited range of 80–100 μmol L^{-1} across a gradient of bloom conditions (Fig. 5I), lower than observed at Wisconsin Point and especially lower than in any of the rivers, where concentrations often exceeded 400 μmol L^{-1} (Fig. 5D).

Particulate stoichiometry shifted with chlorophyll concentration during the bloom with a higher C : P at higher chlorophyll, so a greater deficiency of P during peak bloom (Fig. 6A; Table 4). C : P during the highest chlorophyll concentrations was above ranges typically observed in the lake near- or offshore and is well into the range considered to be indicative of severe P limitation (Fig. 6B). In contrast, C : N was lower at higher chlorophyll. N deficiency was not indicated at high

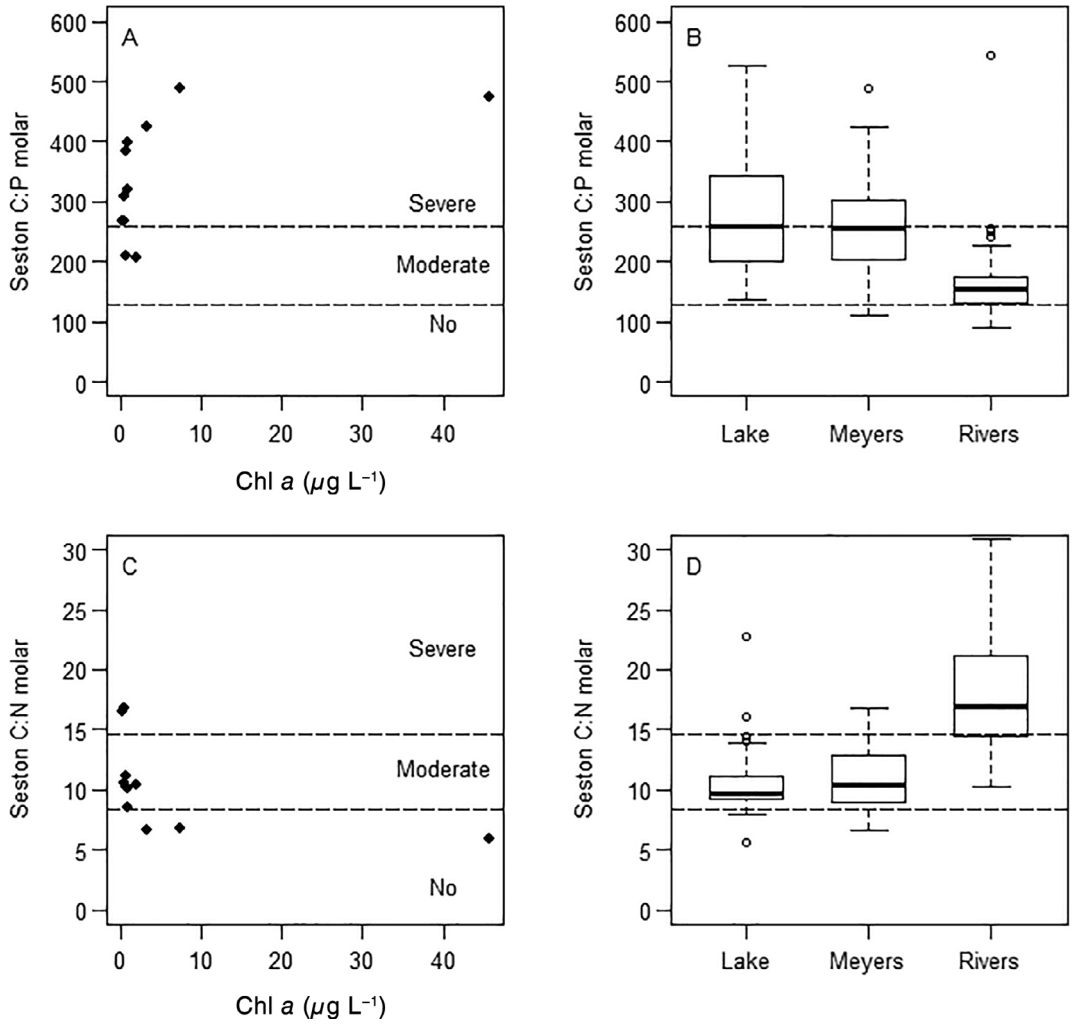

Fig. 6. Ratios of particulate C : P (**A**, **B**) and C : N (**C**, **D**) in the lake nearshore for August 2018 (**A**, **C**) and in environments indicated (**B**, **D**). Boundaries between "No," "Moderate," and "Severe" nutrient deficiency correspond to Guildford and Hecky (2000).

chlorophyll concentration in the bloom (Fig. 6C; Table 4) and it was lower than typically observed in the lake near- or offshore (Fig. 6D). River particles tend to be low in C : P thus enriched in P relative to lake particles (Fig. 6B) and deficient in N compared to in the lake (Fig. 6D).

Toxins

Two of the 11 samples analyzed from the 2018 bloom exhibited toxin values above detection limits of 0.1 $\mu g\ L^{-1}$ (Supporting Information Table S1). An anabaenopeptin (AptA) was detected in the nearshore of the lake on the date and at and near the location where chlorophyll was observed at its highest level. While these 22 toxins are the most commonly measured cyanotoxins in the Great Lakes, we cannot rule out the potential that other cyanotoxins or other congeners of these toxin classes were present.

Discussion

This is the first scientific documentation of the presence of nearshore cyanobacterial blooms along a portion of the southern shoreline of Lake Superior, a region where human recreational contact often is high. The lack of scientific monitoring of this portion of the nearshore from before the first bloom report make it open to interpretation whether cyanobacterial blooms are truly new phenomena in Lake Superior. Attempts to use historic remote sensing images to extend the timeframe backward have been unsuccessful due to the small size of these blooms, their brief durations, and the scarcity of information for ground truthing. Paleolimnological approaches could potentially be used but identifying depositional zones containing usable records in the high-energy nearshore is a challenge. The data available document some of the key characteristics of these blooms, and examination of available historical data, in conjunction with monitoring key chemical and physical attributes during one bloom season, provide some insight into possible factors that may be contributing to the occurrence of these surprising blooms. The context of these blooms in oligotrophic Lake Superior, which is not clearly subjected to high nutrient loadings from agriculture or urbanization, also adds to their general scientific interest, as does the proliferation of diazotrophic cyanobacterial blooms at unusually high N : P ratio. *Dolichospermum* blooms in Lake Superior differ in key characteristics from blooms elsewhere in the Great Lakes. They are not associated with a single, high-nutrient river, and the blooms occur along an exposed shoreline and not in a basin or bay, so it seems that there are multiple factors promoting cyanobacterial blooms in the Great Lakes. In short, occurrence of cyanobacterial blooms in this lake is notable both for scientific and social reasons.

Based on the quantitative data from 2017 and other qualitative microscopic analysis of bloom events in 2012, 2016, and 2018, Lake Superior cyanobacterial blooms beyond the Duluth-Superior harbor are dominated by *D. lemmermanii*. Traits offering *Dolichospermum* advantages over other phytoplankton include buoyancy, formation of heterocysts for N fixation, and survival via akinetes. *Dolichospermum* blooms have been growing in extent in the large lakes of the Southern Alps since 1990s (Salmaso et al. 2015). Blooms of different taxonomic composition were observed in 14 lakes in central and southern Chile and of all cyanobacterial taxa, *Dolichospermum* was found at warmest temperature (15–25°C), deepest euphotic zone depth (3–19 m), lowest TN (< 50 $\mu mol\ L^{-1}$), lowest TP (< 1.3 $\mu mol\ L^{-1}$), lowest conductivity (< 3000 $\mu S\ cm^{-1}$), and moderate pH (7.3–8.5) (Almanza et al. 2019, fig. 4). In the Lake Erie central basin, high abundance of *Dolichospermum* was associated especially with high NO_3^- and high N : P ratios (Chaffin et al. 2019), conditions similar to those where Lake Superior blooms have occurred. In a study of >1000 U.S. lakes, both nutrients and temperature were related to the percent biovolume made up by *Dolichospermum* (referred to there under its former name, *Anabaena*) (Rigosi et al. 2014). A bloom of *Dolichospermum* also was recently reported in the nearshore of Lake Baikal in 2016 (Namsaraev et al. 2018). Peak chlorophyll concentrations in Baikal were similar to those described here in Lake Superior; supporting chemical data were not reported for the Baikal event, but evidence was offered that buoyancy and drift to shore were involved in bloom buildup. The role that akinetes play in Lake Superior blooms has not yet been ascertained, but they may be important in overwintering or in initiating lake blooms (Carey et al. 2009).

Toxin status bears continued examination, but concentration of one potentially toxic congener was observed to be above detection limits in the peak of the bloom. Anabaenopeptin was detected at relatively low concentrations in two samples from the maximum bloom extent. Anabaenopeptins have been described as bioactive compounds potentially useful in pharmaceutical development. Recent evidence suggests they may present some toxicity. For example, they have been shown to be toxic to the nematode *Caenorhabditis elegans* causing shortening life span, delayed hatching, and defects in vulval integrity (Lenz et al. 2019).

The role of climate change is especially important to consider in Lake Superior because it is a rapidly warming lake (Austin and Colman 2008). Summer surface temperature in deep and cold lakes like Lake Superior can rise rapidly in response to climate warming, indeed faster than air temperature due in part to shifting timing of stratification (Woolway and Merchant 2017), making lakes like Superior especially sensitive to climate warming. Summer surface temperature in Lake Superior is responsive to several climate variables (e.g., previous winter's ice cover, air temperature, and wind speed) (Austin and Allen 2011). Warming trends are strongest in the deeper regions of large lakes (Mason et al. 2016; Woolway and Merchant 2018) and warming in the nearshore of Lake Superior is less apparent than in the deeper offshore (Mason et al. 2016).

Signs of change in the primary producers in Lake Superior as a response to warming have been noted previously by others. Increasing relative abundance of *Cyclotella sensu lato* in Lake Superior sediment cores in recent decades have been attributed to warming (Reavie et al. 2016) as has an increase in primary production inferred with $\delta^{13}C$ (O'Beirne et al. 2015). We saw here that Lake Superior cyanobacterial blooms occurred only in seasons where DD were at the high end of the observed range, a product of warming occurring relatively early in the season so affecting the length of the potential growing season. Cyanobacteria, like many phytoplankton, exhibit highest maximal (nutrient-saturated) growth rates at relatively warm temperature. Though not located in the most rapidly warming part of Lake Superior, it is possible that the nearshore has warmed sufficiently to induce blooms, or that shallow embayments or coves may provide particularly changeable zones for warming.

The portion of the nearshore zone subject to blooms is slightly more eutrophic than most of the lake's nearshore zone, so it is plausible that it might be more responsive to increases in nutrient delivery from the land. However, that the appearance of cyanobacterial blooms in Lake Superior is driven solely by increased nutrient loads seems unlikely. Changing land use does not seem to be a factor because land use types associated with nutrient loading have remained a small fraction of the watershed. Algal pigments measured in sediment cores from the St. Louis River estuary (the largest water source to the western part of the lake) did reveal increases in two cyanobacterial pigments (aphanizophyll and myxoxanthophyll) in the upper harbor (above the WWTP outflow) beginning in ~ 1970, with particularly high concentrations since 2000 (Alexson et al. 2018). Long-term records of loading from the smaller rivers such as the Bois Brule are not available, but water quality in the major river source to western Lake Superior (the St. Louis River) has been improving over time. On balance, new point or nonpoint sources of nutrient pollution are not easily identified here as a likely driver for enhanced cyanobacterial blooms.

Extremely large rainstorms have been coincident with major blooms. If storms deliver highly bioavailable nutrients to nearshore zones, a rapid phytoplankton bloom may be expected. In Lake Superior, blooms occur weeks after extreme storms, but generally within hydraulic residence times for this nearshore zone. This temporal lag between loading and blooms bears similarity to Lake Erie where loading of less available storm-derived nutrients may fuel phytoplankton blooms only after a delay of weeks–months (Stumpf et al. 2012). A late May extreme rainfall event was implicated in the large Lake Erie bloom in mid-July 2011 (Michalak et al. 2013). A 45-d delay between storm plume and phytoplankton bloom also has been reported in Lake Pontchartrain (Mishra and Mishra 2010).

Intense, brownish sediment plumes are common in this part of Lake Superior after large rainstorms. Following the June 2012 storm, the sediment plume exhibited elevated TSS, CDOM, TP and SRP, and reduced light compared to out of the plume, but there was little difference in Chl *a*. Elevated P lasted for approximately 1 month (Minor et al. 2014; Cooney et al. 2018). Another large storm event, in 2016, also produced a significant plume with higher CDOM, several forms of carbon (Total Inorganic Carbon, TIC; TOC, DOC), reduced pH, and elevated NH_3, but no change in P compared to the non-plume lake (Cooney et al. 2018). Also pertaining to the 2016 storm, Delvaux (2017) examined a nearshore–offshore transect located in the Apostle Islands and found that 2 weeks after the 2016 storm, P and conductivity were elevated below surface (depth of 5–10 m),whereas DOC was elevated at the surface, suggesting a combination of tributary discharge plus resuspension might have affected nearshore lake chemistry. He saw little to no correspondence of chlorophyll to this plume event, but did observe a shift to heterotrophy (based on reduced production and small increase in respiration) within river plumes, and observed that phytoplankton productivity was stimulated several weeks later. In all these Lake Superior plume studies, there is a suggestion of a mismatch between storm effects on nutrients (increasing them) and light (decreasing it), with offsetting effects on phytoplankton within the plume. How or indeed whether these rainfall events trigger blooms, not immediately, but after a multiple week delay, is presently uncertain but the chance that they import propagules or nutrients to the lake must be considered further.

The high concentrations of both TP and TN observed in Lake Superior bloom waters, with values well above those in inflowing river source waters provides a clear illustration of how cyanobacteria may not just react to, but drive nutrient cycling. Elevated C : P ratios in the bloom suggest that P may have limited *Dolichospermum* growth. This stoichiometry contrasts with the western basin of Lake Erie, where N limits the bloom extent (Chaffin et al. 2013). Vertical translocation of nutrients from sediment nutrient pools into surface phytoplankton blooms and vertical and horizontal hydrodynamic concentration of phytoplankton biomass based on buoyancy and shoreline concentration appear likely in these Lake Superior blooms, perhaps also similar to those processes modeled by Huisman et al. (2004).

This nearshore zone where blooms occur exhibits some different concentrations in multiple substances compared to water further offshore (Fig. 5), indicating continuous mixing of river and lake water in this zone. However, the fact that both DOC and Si in the August 2018 bloom were very similar to concentrations observed in nearby nonbloom lake water indicates that the bloom biomass was not inhabiting distinct river plume water. So though rivers may be involved in early bloom formation, exchange between rivers and lake waters is important to understand. On the other hand, both N and P in the bloom were many times more concentrated than in the lake or any potential source water. This difference strongly

suggests an important role for hydrodynamic concentration of cyanobacterial biomass in these blooms. Positive buoyancy, coupled with prevailing longshore currents and unique geoform features (e.g., the shore itself plus minor embayments) likely help explain how blooms achieve the high concentration that they do in this part of the lake as well as the short duration of bloom events. Hydrodynamic concentration seems to be an insufficient explanation by itself though because major blooms of *Dolichospermum* in this location are undocumented prior to 2012, suggesting though not proving they are a recent phenomenon. Stoichiometric patterns with phytoplankton biomass indicate no sign of N limiting blooms, and in the presence of NO_3^- and high TN : TP, it is not at all likely that competition for N is an important factor, but the bloom extent may be limited by P.

Cyanobacterial blooms can now be said to occur in all five of the Laurentian Great Lakes. It is notable that dense cyanobacterial populations in Lake Superior were not anticipated by scientists or managers, and they threaten a high value resource, so it is critical to assess as quickly as possible their triggers and characteristics so management options can be evaluated. There are several priorities to improve our understanding of cyanobacterial blooms in this oligotrophic lake. Two that build directly on the present study are: (1) improved monitoring of this nearshore environment and associated tributaries and (2) mechanistic, experimental studies of bloom drivers. In addition, overcoming challenges to using remote sensing in this temporally dynamic and small nearshore zone would be beneficial as would identifying suitable locations and performing paleolimnological studies of cyanobacteria presence in the nearshore. In summary, the evidence summarized here suggests that during peak temperature in years with long growing seasons, and in years of extreme rainfall events, *Dolichospermum* in Lake Superior grow sufficiently to be concentrated by buoyancy and hydrodynamics into cyanobacterial blooms at the shoreline where recreational values and human contact are high. These findings point to lake warming and other climate drivers as promoting cyanobacterial blooms in Lake Superior.

References

Alexson, E. E., E. D. Reavie, R. P. Axler, S. V. Yemets, P. A. Krasuntsky, M. B. Edlund, R. W. Pillsbury, and D. Desotelle. 2018. Paleolimnology of a freshwater estuary to inform Area of Concern nutrient delisting efforts. J. Paleolimnol. **59**: 373–395. doi:10.1007/s10933-017-0014-8

Almanza, V., P. Pederos, H. D. Laughinghouse IV, J. Feléz, O. Parra, M. Azócar, and R. Urrutia. 2019. Association between trophic state, watershed use, and blooms of cyanobacteria in south-central Chile. Limnologica **75**: 30–41. doi:10.1016/j.limno.2018.11.004

Austin, J. A. 2013. The potential for autonomous underwater gliders in large lake research. J. Great Lakes Res. **39**: 8–13. doi:10.1016/j.jglr.2013.01.004

Austin, J. A., and S. M. Colman. 2008. A century of temperature variability in Lake Superior. Limnol. Oceanogr. **53**: 2724–2730. doi:10.4319/lo.2008.53.6.2724

Austin, J. A., and J. Allen. 2011. Sensitivity of summer Lake Superior thermal structure to meteorological forcing. Limnol. Oceanogr. **56**: 1141–1154. doi:10.4319/lo.2011.56.3.1141

Bartlett, S. L., S. L. Brunner, J. V. Klump, E. M. Houghton, and T. R. Miller. 2018. Spatial analysis of toxic or otherwise bioactive cyanobacterial peptides in Green Bay, Lake Michigan. J. Great Lakes Res. **44**: 924–933. doi:10.1016/j.jglr.2018.08.016

Bellinger, B. J., and others. 2016. Water quality in the St. Louis River Area of Concern, Lake Superior: Historical and current conditions and delisting implications. J. Great Lakes Res. **42**: 28–38. doi:10.1016/j.jglr.2015.11.008

Beversdorf, L., C. Weirich, S. Bartlett, and T. Miller. 2017. Variable cyanobacterial toxin and metabolite profiles across six eutrophic lakes of differing physiochemical characteristics. Toxins **9**: 62. doi:10.3390/toxins9020062

Bramburger, A. J., and E. D. Reavie. 2016. A comparison of phytoplankton communities of the deep chlorophyll layers and epilimnia of the Laurentian Great Lakes. J. Great Lakes Res. **42**: 1016–1025. doi:10.1016/j.jglr.2016.07.004

Carey, C. C., K. C. Weathers, and K. L. Cottingham. 2009. Increases in phosphorus at the sediment-water interface may influence the initiation of cyanobacterial blooms in an oligotrophic lake. Int. Ver. Theor. Angew. Limnol. Verh. **30**: 1185–1188. doi:10.1080/03680770.2009.11923908

Carey, C. C., H. A. Ewing, K. L. Cottingham, K. C. Weathers, R. Q. Thomas, and J. F. Haney. 2012. Occurrence and toxicity of the cyanobacterium *Gloeotrichia echinulata* in low-nutrient lakes in the northeastern United States. Aquat. Ecol. **46**: 395–409. doi:10.1007/s10452-012-9409-9

Chaffin, J. D., T. B. Bridgeman, and D. L. Bade. 2013. Nitrogen constrains the growth of late summer cyanobacterial blooms in Lake Erie. Adv. Microbiol. **3**: 16–26. doi:10.4236/aim.2013.36A003

Chaffin, J. D., and others. 2019. Cyanobacterial blooms in the central basin of Lake Erie: Potentials for cyanotoxins and environmental drivers. J. Great Lakes Res. **45**: 277–289. doi:10.1016/j.jglr.2018.12.006

Cooney, E. M., P. Mckinney, R. W. Sterner, G. E. Small, and E. C. Minor. 2018. Tale of two storms: Impact of extreme rain events on the biogeochemistry of Lake Superior. J. Geophys. Res. Biogeosci. **123**: 1719–1731. doi:10.1029/2017JG004216

Delvaux, J. 2017. River influence on the nearshore ecosystem of western Lake Superior. Master of Science. Univ. of Wisconsin Milwaukee.

Guildford, S. J., and R. E. Hecky. 2000. Total nitrogen, total phosphorus, and nutrient limitation in lakes and oceans: Is there a common relationship? Limnol. Oceanogr. **45**: 1213–1223. doi:10.4319/lo.2000.45.6.1213

Ho, J. C., A. M. Michalak, and N. Pahlevan. 2019. Widespread global increase in intense lake phytoplankton blooms since the 1980s. Nature **574**: 667–670. doi:10.1038/s41586-019-1648-7

Huisman, J., J. Sharples, J. M. Stroom, P. M. Visser, W. E. A. Kardinaal, J. M. H. Verspagen, and B. Sommeijer. 2004. Changes in turbulent mixing shift competition for light between phytoplankton species. Ecology **85**: 2960–2970. doi:10.1890/03-0763

Kemp, A. L. W., C. I. Dell, and N. S. Harper. 1978. Sedimentation rates and a sediment budget for Lake Superior. J. Great Lakes Res. **4**: 276–287. doi:10.1016/S0380-1330(78)72198-2

Lenz, K. A., T. R. Miller, and H. Ma. 2019. Anabaenopeptins and cyanopeptolins induce systemic toxicity effects in a model organism the nematode *Caenorhabditis elegans*. Chemosphere **214**: 60–69. doi:10.1016/j.chemosphere.2018.09.076

Mason, L. A., and others. 2016. Fine-scale spatial variation in ice cover and surface temperature trends across the surface of the Laurentian Great Lakes. Clim. Change **138**: 71–83. doi:10.1007/s10584-016-1721-2

McKinney, P., K. S. Tokos, and K. Matsumoto. 2018. Modeling nearshore-offshore exchange in Lake Superior. PLoS One **13**: e0193183. doi:10.1371/journal.pone.0193183

Michalak, A. M., and others. 2013. Record-setting algal bloom in Lake Erie caused by agricultural and meteorological trends consistent with expected future conditions. Proc. Natl. Acad. Sci. USA **110**: 6448–6452. doi:10.1073/pnas.1216006110

Millie, D., G. L. Fahnenstiel, J. Dyble, R. Pigg, R. Rediske, D. M. Klarer, R. W. Litaker, and P. A. Tester. 2008. Influence of environmental conditions on late-summer cyanobacterial abundance in Saginaw Bay, Lake Huron. Aquat. Ecosyst. Health Manag. **11**: 196–205. doi:10.1080/14634980802099604

Minor, E. C., B. Forsman, and S. J. Guildford. 2014. The effect of a flood pulse on the water column of western Lake Superior, USA. J. Great Lakes Res. **40**: 455–462. doi:10.1016/j.jglr.2014.03.015

Mishra, D. R., and S. Mishra. 2010. Plume and bloom: Effect of the Mississippi River diversion on the water quality of Lake Pontchartrain. Geocarto Int. **25**: 555–568. doi:10.1080/10106041003763394

Namsaraev, Z., A. Melnikova, V. Ivanov, A. Komova, and A. Teslyuk. 2018. Cyanobacterial bloom in the world largest freshwater Lake Baikal. IOP Conf. Ser. Earth Environ. Sci. **121**: 032039. doi:10.1088/1755-1315/121/3/032039

O'Beirne, M. D., L. J. Strzok, J. P. Werne, T. C. Johnson, and R. E. Hecky. 2015. Anthropogenic influences on the sedimentary geochemical record in western Lake Superior (1800–present). J. Great Lakes Res. **41**: 20–29. doi:10.1016/j.jglr.2014.11.005

Paerl, H. W., and T. G. Otten. 2013. Harmful cyanobacterial blooms: Causes, consequences, and controls. Microb. Ecol. **65**: 995–1010. doi:10.1007/s00248-012-0159-y

Perri, K. A., J. M. Sullivan, and G. L. Boyer. 2015. Harmful algal blooms in Sodus Bay, Lake Ontario: A comparison of nutrients, marina presence, and cyanobacterial toxins. J. Great Lakes Res. **41**: 326–337. doi:10.1016/j.jglr.2015.03.022

Planet Team. 2017. Planet application program interface: In space for life on Earth. Available from https://api.planet.com

Reavie, E. D., R. P. Barbiero, L. E. Allinger, and G. J. Warren. 2014. Phytoplankton trends in the Laurentian Great Lakes: 2001-2014. J. Great Lakes Res. **40**: 618–639. doi:10.1016/j.jglr.2014.04.013

Reavie, E. D., and others. 2016. Climate warming and changes in *Cyclotella sensu lato* in the Laurentian Great Lakes. Limnol. Oceanogr. **62**: 768–783. doi:10.1002/lno.10459

Rigosi, A., C. C. Carey, B. W. Ibelings, and J. D. Brookes. 2014. The interaction between climate warming and eutrophication to promote cyanobacteria is dependent on trophic state and varies among taxa. Limnol. Oceanogr. **59**: 99–114. doi:10.4319/lo.2014.59.1.0099

Robertson, D. M. 1997. Regionalized loads of sediment and phosphorus to Lakes Michigan and Superior—high flow and long-term average. J. Great Lakes Res. **23**: 416–439. doi:10.1016/S0380-1330(97)70923-7

Russ, M. E., N. E. Ostrom, H. Gandhi, P. H. Ostrom, and N. R. Urban. 2004. Temporal and spatial variations in R:P ratios in Lake Superior, an oligotrophic freshwater environment. J. Geophys. Res. Oceans **109**: C10S12. doi:10.1029/2003JC001890

Salmaso, N., C. Capelli, S. Shams, and L. Cerasino. 2015. Expansion of bloom-forming *Dolichospermum lemmermannii* (Nostocales, Cyanobacteria) to the deep lakes south of the Alps: Colonization patterns, driving forces and implications for water use. Harmful Algae **50**: 76–87. doi:10.1016/j.hal.2015.09.008

Sterner, R. W. 2011. C:N:P stoichiometry in Lake Superior: Freshwater sea as end member. Inland Waters **1**: 29–46. doi:10.5268/IW-1.1.365

Sterner, R. W., T. M. Smutka, R. M. L. McKay, Q. Xiaoming, E. T. Brown, and R. M. Sherrell. 2004. Phosphorus and trace metal limitation of algae and bacteria in Lake Superior. Limnol. Oceanogr. **49**: 495–507. doi:10.4319/lo.2004.49.2.0495

Stumpf, R. P., T. T. Wynne, D. B. Baker, and G. L. Fahnenstiel. 2012. Interannual variability of cyanobacterial blooms in Lake Erie. PLoS One **7**: e42444. doi:10.1371/journal.pone.0042444

Taylor, B. W., and others. 2007. Improving the fluorometric ammonium method: Matrix effects, background fluorescence, and

standard additions. J. North. Am. Benthol. Soc. **26**: 167–177. doi:10.1899/0887-3593(2007)26[167:ITFAMM]2.0.CO;2

Tonello, M. S., T. S. Hebner, R. W. Sterner, S. Brovold, T. Tiecher, E. C. Boroluzzi, and G. H. Merten. 2019. Geochemistry and minerology of southwestern Lake Superior sediments with an emphasis on phosphorus lability. J. Soils Sediments **20**: 1060–1073. doi:10.1007/s11368-019-02420-5

Tromas, N., N. Fortin, L. Bedrani, Y. Terrat, P. Cardoso, D. Bird, C. W. Greer, and B. J. Shapiro. 2017. Characterising and predicting cyanobacterial blooms in an 8-year amplicon sequencing time course. ISME J. **11**: 1746–1763. doi:10.1038/ismej.2017.58

Watson, S. B., and others. 2016. The re-eutrophication of Lake Erie: Harmful algal blooms and hypoxia. Harmful Algae **56**: 44–66. doi:10.1016/j.hal.2016.04.010

Welschmeyer, N. A. 1994. Fluorometric analysis of chlorophyll *a* in the presence of chlorophyll *b* and pheopigments. Limnol. Oceanogr. **39**: 1985–1992. doi:10.4319/lo.1994.39.8.1985

author>Winter, J. G., A. M. DeSallas, R. Fletcher, L. Heintsch, A. Moreley, L. Nakamoto, and K. Utsumi. 2011. Algal blooms in Ontario, Canada: Increases in reports since 1994. Lake Reserv. Manag. **27**: 107–114. doi:10.1080/07438141.2011.557765

Woolway, R. L., and C. J. Merchant. 2017. Amplified surface temperature response of cold, deep lakes to inter-annual air temperature variability. Sci. Rep. **7**: 4130. doi:10.1038/s41598-017-04058-0

Woolway, R. I., and C. J. Merchant. 2018. Intralake heterogeneity of thermal responses to climate hange: A xtudy of large northern hemisphere lakes. J. Geophys. Res. Atmos. **123**: 3087–3098. doi:10.1002/2017jd027661

Xue, P., D. J. Schwab, and S. Hu. 2015. An investigation of the thermal response to meteorological forcing in a hydrodynamic model of Lake Superior. J. Geophys. Res. Oceans **120**: 5233–5253. doi:10.1002/2015JC010740

Yang, L., and others. 2018. A new generation of the United States National Land Cover Database: Requirements, research priorities, design, and implementation strategies. ISPRS J. Photogramm. Remote Sens. **146**: 108–123. doi:10.1016/j.isprsjprs.2018.09.006

Yurista, P., J. R. Kelly, and S. E. Miller. 2011. Lake Superior: Nearshore variability and a landscape driver concept. Aquat. Ecosyst. Health Manag. **14**: 345–355. doi:10.1080/14634988.2011.624942

Acknowledgments

Financial support was provided by The University of Minnesota Duluth and the National Park Service via the Great Lakes Restoration Initiative. KLR received partial financial support from the Cooperative Institute for Great Lakes Research. The Great Lakes Observing System (GLOS) provided funding to support the LLO1 and LLO2 buoys. Field and lab assistance was provided by Nicole Farley and Madison Perry as well as Theodore Gostomski, David VanderMeulen, and Jay Glase. We thank Gina LaLiberte, Wisconsin Department of Natural Resources, for her assistance with phytoplankton identification and for providing photomicrographs. We also thank H. Bootsma and J. Delvaux from the University of Wisconsin Milwaukee for 2015–2016 APIS temperature data.

Conflict of Interest

None declared.

Submitted 11 June 2019
Revised 04 November 2019
Accepted 02 July 2020

Associate editor: Michelle McCrackin